# A GENTLE INTRODUCTION TO THE PHYSICS OF SPECTRAL LINE POLARIZATION

JAVIER TRUJILLO BUENO
*Instituto de Astrofísica de Canarias, 38205 La Laguna, Tenerife, Spain*

**Abstract.** This paper presents a pedagogical introduction to the physical mechanisms that produce spectral line polarization in stellar atmospheres, emphasizing the importance of developing reliable diagnostic tools that take proper account of the Zeeman and Paschen-Back effects, scattering polarization and the Hanle effect. Only in this way may we hope to investigate the complexity of solar and stellar magnetic fields in a parameter domain that goes from field intensities as low as one milligauss to many thousands of gauss.

**Key words:** polarization, scattering, solar and stellar magnetic fields

## 1. Introduction

The state of polarization of a quasi-monochromatic beam of electromagnetic radiation can be conveniently characterized in terms of four quantities that can be measured by furnishing our telescopes with a polarimeter. Such observables are the four Stokes parameters $(I, Q, U, V)$, which were formulated by Sir George Stokes in 1852 and introduced into astrophysics by the Nobel laureate Subrahmanyan Chandrasekhar in 1946. The Stokes $I(\lambda)$ profile represents the intensity as a function of wavelength, Stokes $Q(\lambda)$ the *intensity difference* between vertical and horizontal linear polarization, Stokes $U(\lambda)$ the intensity difference between linear polarization at $+45°$ and $-45°$, while Stokes $V(\lambda)$ the intensity difference between right- and left-handed circular polarization (cf. Born & Wolf, 1994). Note that the definition of the Stokes $Q$ and $U$ parameters requires first choosing a reference direction for $Q > 0$ in the plane perpendicular to the direction of propagation.

Let us now introduce the most important mechanisms that induce (and modify) polarization signatures in the spectral lines that originate in stellar atmospheres: the Zeeman and Paschen-Back effects, scattering processes and the Hanle effect.

## 2. The Zeeman effect

As illustrated in Figure 1, the Zeeman effect requires the presence of a magnetic field which causes the atomic and molecular energy levels to split into different magnetic sublevels characterized by their magnetic quantum number $M$ (Condon & Shortley, 1935). Each level of total angular momentum $J$ splits into $(2J + 1)$ sublevels, the splitting being proportional to the level's Landé factor, $g_J$, and to the magnetic field strength. As a result, a spectral line between a lower level with $(J_l, g_l)$ and an upper level with $(J_u, g_u)$ is composed of several individual components whose frequencies are given by $\nu_{J_l M_l}^{J_u M_u} = \nu_0 + \nu_L(g_u M_u - g_l M_l)$, where $\nu_0$ is the frequency

of the line in the absence of magnetic fields and $\nu_L = 1.3996 \times 10^6 B$ is the Larmor frequency (with $B$ the magnetic field strength expressed in gauss). In particular, a line transition with $J_l = 0$ and $J_u = 1$ has three components (see Fig. 1): one $\pi$ component centered at $\nu_0$ (or at $\lambda_0$), one $\sigma_{\rm red}$ component centered at $\nu_0 - g_u\nu_L$ (or at $\lambda_0 + g_u\Delta\lambda_B$), and one $\sigma_{\rm blue}$ component centered at $\nu_0 + g_u\nu_L$ (or at $\lambda_0 - g_u\Delta\lambda_B$), where $\Delta\lambda_B = 4.6686 \times 10^{-13}\lambda_0^2 B$ (with $\lambda_0$ in Å and $B$ in gauss).
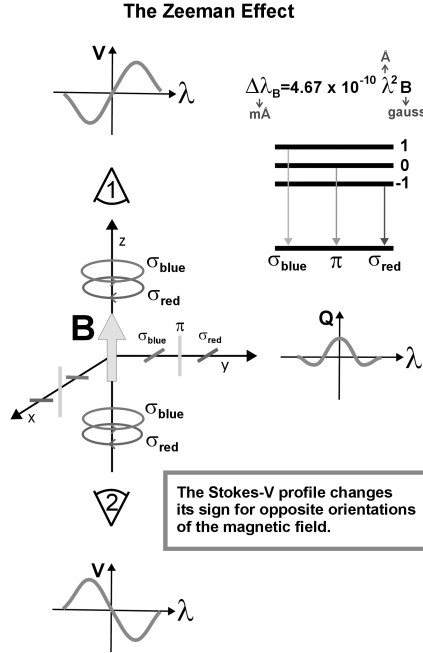


Fig. 1.     The oscillator model for the Zeeman effect indicating the characteristic shapes of the circular and linear polarization profiles as generated locally via the emission process. It is important to note that the Stokes $V(\lambda)$ profile changes its sign for opposite orientations of the magnetic field vector, while the Stokes $Q(\lambda)$ profile reverses sign when the transverse field component is rotated by $\pm 90°$.

The important point to remember is that the polarization signals produced by the Zeeman effect are caused by the *wavelength shifts* between the $\pi$ ($\Delta M = M_u - M_l = 0$) and $\sigma_{b,r}$ ($\Delta M = \pm 1$) transitions. Such wavelength shifts are also the physical origin of the spectral line polarization induced by the Paschen-Back effect discussed below in Section 7, since the only difference with respect to the linear Zeeman effect theory considered here lies in the calculation of the positions and strengths of the various $\pi$ and $\sigma$ components.

The Zeeman effect is most sensitive in circular polarization (quantified by the Stokes $V$ parameter), with a magnitude that for not too strong fields scales with the ratio between the Zeeman splitting and the width of the spectral line (which is very much larger than the natural width of the atomic levels!), and in such a way that the emergent Stokes $V(\lambda)$ profile changes its sign for opposite orientations

of the magnetic field vector. This so-called *longitudinal* Zeeman effect responds to the line-of-sight component of the magnetic field. Accordingly, if we have a perfect cancellation of mixed magnetic polarities within the spatio-temporal resolution element of the observation, the measured circular polarization would be exactly zero *if* the thermodynamic and dynamic properties of the mixed magnetic components are similar. The antisymmetric shape of the Stokes $V(\lambda)$ profiles illustrated in Fig. 1 can be easily understood by noting the expression of the Stokes-$V$ component of the emission vector:

$$\epsilon_V = \frac{h\nu}{4\pi} N_u A_{ul} \frac{1}{2} [\phi_{\text{red}} - \phi_{\text{blue}}] \cos\theta, \qquad (1)$$

where $\theta$ is the angle between the magnetic field vector and the line of sight, $A_{ul}$ the Einstein coefficient for the spontaneous emission process, $N_u$ the number of atoms per unit volume in the upper level of the line transition under consideration, while $\phi_{\text{red}}$ and $\phi_{\text{blue}}$ are profiles that result from the superposition of the Voigt functions corresponding to each individual component. $\phi_{\text{red}}$ is displaced to the red side of the central wavelength $\lambda_0$, and $\phi_{\text{blue}}$ to the blue side. For instance, for the particular case of a line transition with $J_l = 0$ and $J_u = 1$, $\phi_{\text{red}}$ is a Voigt profile centered at $\lambda_0 + g_u \Delta\lambda_B$ and $\phi_{\text{blue}}$ a Voigt profile centered at $\lambda_0 - g_u \Delta\lambda_B$.

In contrast, the *transverse* Zeeman effect responds to the component of the magnetic field perpendicular to the line of sight, but produces linear polarization signals (quantified by the Stokes $Q$ and $U$ parameters) that are normally below the noise level of present observational possibilities for intrinsically weak fields (typically B < 100 gauss for solar spectropolarimetry). The Stokes $Q$ and $U$ profiles induced by the Zeeman effect at a given point in a magnetized plasma have a three-lobe shape which is also illustrated in Fig. 1. This characteristic shape can be easily understood by noting that the expression of the Stokes-$Q$ component of the emission vector is:

$$\epsilon_Q = \frac{h\nu}{4\pi} N_u A_{ul} \frac{1}{2} [\phi_\pi - (\frac{\phi_{\text{red}} + \phi_{\text{blue}}}{2})] \sin^2\theta \cos 2\chi, \qquad (2)$$

where $\chi$ is the angle that the projection line of the magnetic field vector on the plane perpendicular to the direction of propagation forms with the reference direction chosen for $Q > 0$.

Figure 2 shows an interesting example of Stokes profiles produced by the solar atmospheric plasma. The top panel is a section of the Fraunhofer spectrum between 4602 Å and 4610 Å showing the familiar absorption lines corresponding to several chemical elements. The remaining panels give the fractional polarizations $X(\lambda)/I(\lambda)$ (with $X = Q, U, V$). The spectrograph slit was placed parallel to and 2.5 arcsec inside the limb (at $\mu = 0.07$, where $\mu$ is the cosine of the heliocentric angle), such that half of the slit covers a significantly magnetized region, while the other half lies outside it. In the magnetically active region (which corresponds to the lower half of each of the four panels of Fig. 2) we see the characteristic signatures of the Zeeman effect. The $V/I$ panel shows the typical antisymmetric signature of the longitudinal Zeeman effect with a positive and a negative lobe for each spectral line, while in the lower half of the panels for $Q/I$ and $U/I$ we see the typical symmetric signature of the transverse Zeeman effect with two lobes in the wings of opposite sign to the central lobe. Interestingly, as soon as we go outside the facular region (see the upper

half of each of the four panels in Fig. 2) we see that the amplitude of the circular polarization is significantly reduced in all atomic lines, while practically the only existing linear polarization signal is the $Q/I$ peak corresponding to the Sr I line at 4607 Å . However, the shape of this $Q/I$ profile is Gaussian-like, suggesting that it is not produced by the transverse Zeeman effect. If it does not result from the Zeeman effect, what, then, could its physical origin be?
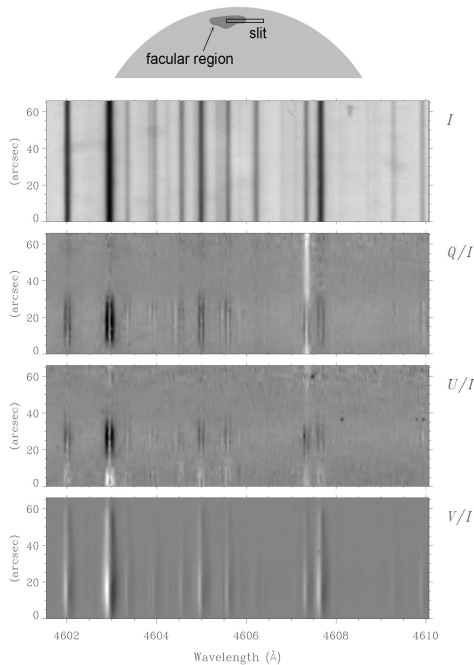


Fig. 2.    Spectropolarimetric observation close to the edge of the solar disk with half of the spectrograph slit crossing a moderately magnetized facular region. Note that while the characteristic signature of the longitudinal Zeeman effect is present at all spatial points along the slit, the signature of the transverse Zeeman effect disappears as soon as one goes outside the facular region. Interestingly, the only spectral line which shows linear polarization outside the facular region is the Sr I line at 4607 Å with a $Q/I$ shape that has nothing to do with the transverse Zeeman effect. This spectropolarimetric observation was obtained by Stenflo (2002).

## 3. Atomic level polarization

The amplitudes of polarization signals induced by the Zeeman effect are very small when the Zeeman splitting is a very small fraction of the spectral line width. If there is no Zeeman splitting, there is no wavelength shift between the $\pi$ and $\sigma$ transitions, and there is no measurable polarization because the polarizations of such components cancel out. However, it is easy to see that this is only true if the populations of the magnetic sublevels pertaining to the lower and/or upper levels of the spectral line under consideration are assumed to be identical.

To this end, consider the case of a line transition with $J_l = 0$ and $J_u = 1$ and choose the quantization axis of total angular momentum along the solar radius vector through the observed point. Assume that the population of the upper-level magnetic sublevel with $M_u = 0$ is smaller than the populations of the magnetic sublevels with $M_u = \pm 1$. As a result, even in the absence of a magnetic field (zero Zeeman splitting), we can have a non-zero linear polarization signal, simply because the number of $\sigma$ transitions per unit volume and time will be larger than the ensuing number of $\pi$ transitions. For example, for the case of magnetic field oriented along the solar radius vector through the observed point, a more general expression for the Stokes-$Q$ component of the emission vector would be[1]

$$\epsilon_Q = \frac{h\nu}{4\pi} A_{ul} \frac{3}{2} [\rho_1(0,0)\phi_\pi - (\frac{\rho_1(-1,-1)\phi_{\rm red} + \rho_1(1,1)\phi_{\rm blue}}{2})]\sin^2\theta, \qquad (3)$$

where $\theta$ is the angle between the quantization axis of total angular momentum (chosen here along the solar radius vector through the observed point) and the line of sight, while $\rho_{J_u}(M,M)$ is the population of the upper-level sublevel with magnetic quantum number $M$. This expression shows clearly that in the absence of a magnetic field (i.e., when $\phi_\pi = \phi_{\rm red} = \phi_{\rm blue}$ because their central wavelengths coincide at $\lambda_0$ for $B = 0$ gauss) the Stokes-$Q$ profile is equal to the difference between two Voigt profiles: one (resulting from the $\pi$ transition) centered at $\lambda_0$ and an extra one (resulting from the $\sigma$ transitions) centered also at $\lambda_0$ but of greater amplitude. This is precisely the explanation of the curious linear polarization of the Sr I line seen in Fig. 2, as observed in "quiet" regions close to the edge of the solar disk. Given that this spectral line has $J_l = 0$, its linear polarization is totally due to the *selective emission* processes resulting from the population imbalances of the upper level.

On the other hand, it is very important to understand that whenever the Zeeman splitting is a negligible fraction of the spectral line width, spectral lines with $J_l = 1$ and $J_u = 0$ can produce linear polarization only if there exist population imbalances among the magnetic sublevels of their lower-level. If this is the case, then linear polarization can be generated via the *selective absorption* of polarization components resulting from the population imbalances of the lower level (Trujillo Bueno & Landi Degl'Innocenti, 1997; Trujillo Bueno, 1999, 2001, 2003a; Trujillo Bueno et al., 2002a). The same applies to $J_l = 3/2 \rightarrow J_u = 1/2$ transitions, like the $\lambda 8662$ Å line of the Ca II IR triplet (Manso Sainz & Trujillo Bueno, 2003a). Interestingly, lower-level atomic polarization and the ensuing selective absorption mechanism (i.e., 'zero-field' dichroism) is the physical origin of the 'enigmatic' signals of the linearly-polarized solar limb spectrum (or *second solar spectrum*) which has been discovered recently using novel polarimeters that allow the detection of very low amplitude polarization signals (with $10^{-6} < Q/I < 10^{-3}$; see Stenflo & Keller, 1997; Stenflo et al., 2000; Gandorfer, 2000, 2002).

In summary, spectral line polarization can be produced by the mere presence of *atomic level polarization*, i.e., by the existence of population imbalances among the sublevels pertaining to the upper and/or lower atomic levels involved in the line

---

[1] I have chosen here the positive reference direction for $Q > 0$ such that $\cos 2\chi = 1$.

transition under consideration.[2] Upper-level polarization produces selective emission of polarization components (i.e., the emitted light is polarized, even in the absence of a magnetic field), while lower-level polarization causes selective absorption of polarization components (i.e., the transmitted beam is polarized, even in the absence of a magnetic field).

## 4. Anisotropic radiation pumping

What is the key physical mechanism that induces atomic level polarization in a stellar atmosphere? The answer lies in the *the anisotropic illumination* of the atoms, which produces *atomic alignment.* This is easy to understand by considering the academic case of a unidirectional unpolarized light beam that illuminates a gas of two-level atoms with $J_l = 0$ and $J_u = 1$ and that is propagating along the direction chosen as the quantization axis of total angular momentum. Since these atoms can only absorb $\pm 1$ units of angular momentum from the light beam, only transitions corresponding to $\Delta M = \pm 1$ are effective, so that no transitions occur to the $M = 0$ sublevel of the upper level. Thus, in the absence of any relaxation mechanisms, the upper-level sublevels with $M = 1$ and $M = -1$ would be more populated than the $M = 0$ sublevel and the alignment coefficient $\rho_0^2(J_u = 1) = (N_1 - 2N_0 + N_{-1})/\sqrt{6}$ would have a positive value.

Upper-level selective population pumping occurs when some upper state sublevels have more chance of being populated than others. On the contrary, as illustrated in Fig. 3, lower-level selective depopulation pumping occurs when some lower state sublevels absorb light more strongly than others. As a result, an excess population tends to build up in the weakly absorbing sublevels (Kastler, 1950; Happer, 1972; Trujillo Bueno & Landi Degl'Innocenti, 1997; Trujillo Bueno, 1999, 2001, 2003a; Manso Sainz & Trujillo Bueno, 2003a). It is also important to note that line transitions between levels having other total angular momentum values (e.g., $J_l = J_u = 1$) permit the transfer of atomic polarization between both levels via a process called *re-population pumping* (e.g., lower-level atomic polarization can result simply from the spontaneous decay of a polarized upper level; see Trujillo Bueno et al., 2002b). The presence of a magnetic field is not necessary for the operation of such optical pumping processes, which can be particularly efficient in creating atomic polarization if the depolarizing rates from elastic collisions are sufficiently low. Figure 4 illustrates the type of anisotropic illumination in the outer layers of a stellar atmosphere.

## 5. The Hanle effect: classical description

The Hanle effect is the modification of the atomic-level polarization (and of the ensuing observable effects on the emergent Stokes profiles) caused by the action of a

---

[2] There are two possible types of atomic level polarization: alignment and orientation. Atomic alignment is a condition of population imbalances between the Zeeman substates of a level, such that the total population of substates with different values of $|M|$ are different. One speaks instead of atomic orientation when, for a given value of $|M|$, the substates labeled by M and -M have different populations. Moreover, the concept of atomic polarization includes also the possibility of quantum interferences (or coherences) among the magnetic sublevels of each $J$-level, and even among those belonging to different $J$-levels.
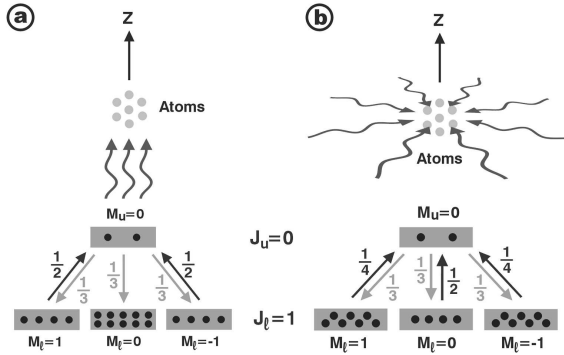
Fig. 3.    Illustration of the atomic polarization that is induced in the lower level of a two-level atom (with $J_l = 1$ and $J_u = 0$) by two types of anisotropic illuminations (**a** and **b**). The incident radiation field is assumed to be unpolarized and with axial symmetry around the vertical direction, which is our choice here for the quantization axis of total angular momentum. In both cases, an excess population tends to build up in the weakly absorbing sublevels. Note that the alignment coefficient of the lower level (i.e. $\rho_0^2 = (N_1 - 2N_0 + N_{-1})/\sqrt{6}$, $N_i$ being the populations of the magnetic sublevels) is negative in case (**a**) (where the incident beam is parallel to the quantization axis), but positive in case (**b**) (where the incident beams are perpendicular to the quantization axis).

magnetic field *inclined* with respect to the symmetry axis of the pumping radiation field. The basic formula to estimate the magnetic field intensity, $B_{\mathrm{H}}$ (measured in gauss), sufficient to produce a sizable change in the atomic level polarization results from equating the Zeeman splitting with the natural width (or inverse lifetime) of the energy level under consideration:

$$B_H = 1.137 \times 10^{-7}/(t_{\mathrm{life}}\, g_J)\,, \tag{4}$$

where $g_J$ and $t_{\mathrm{life}}$ are, respectively, the Landé factor and the level's lifetime (in seconds), which can be either the upper or the lower level of the chosen spectral line. This formula provides a reliable estimation only when radiative transitions dominate completely the atomic excitation. If elastic and/or inelastic collisions are also efficient, then the critical field increases, since it turns out to be approximately given by (Trujillo Bueno, 2003a)

$$B \approx \frac{1 + \delta(1 - \epsilon)}{1 - \epsilon}\, B_H\,, \tag{5}$$

where $\delta = D/A_{ul}$ quantifies the rate of elastic (depolarizing) collisions in units of the Einstein $A_{ul}$-coefficient, and $\epsilon = C_{ul}/(C_{ul} + A_{ul})$ is the probability that a de-excitation event is caused by collisions (with $C_{ul}$ the rate of inelastic collisional transitions between the upper level "$u$" and the lower level "$l$"). The application of this basic equation to the upper and lower levels of typical spectral lines shows that the Hanle effect may allow us to diagnose solar and stellar magnetic fields having intensities between at least one milligauss and a few hundred gauss, i.e., in a parameter domain that is very hard to study via the Zeeman effect alone.
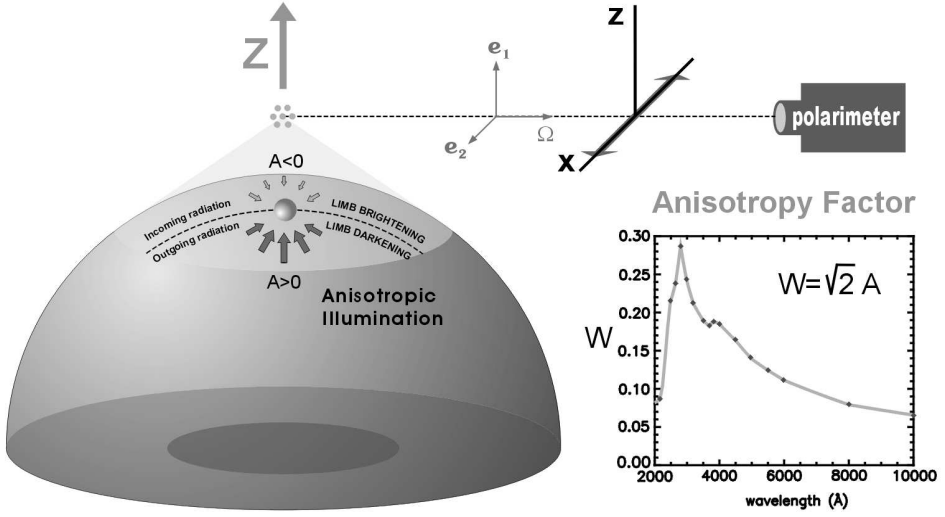
Fig. 4. Anisotropic illumination of the outer layers of a stellar atmosphere, indicating that the outgoing continuum radiation (which shows limb darkening) is predominantly *vertical* while the incoming radiation (which shows limb brightening) is predominantly *horizontal* . The figure also illustrates the type of anisotropic illumination experienced by atoms situated at a given height above the visible 'surface' of the star, including the polarization analysis of the scattered beam at 90°. The 'degree of anisotropy' of the incident radiation field is quantified by $A = J_0^2/J_0^0$, where $J_0^0$ is the familiar mean intensity and $J_0^2 \approx \oint \frac{d\vec{\Omega}}{4\pi} \frac{1}{2\sqrt{2}}(3\mu^2 - 1)I_{\nu,\vec{\Omega}}$ (with $I_{\nu,\vec{\Omega}}$ the Stokes-$I$ parameter as a function of frequency $\nu$ and direction $\vec{\Omega}$, while $\mu = \cos\theta$, with $\theta$ the polar angle with respect to the Z-axis). The possible values of the 'anisotropy factor' $W = \sqrt{2}A$ vary between $W = -1/2$, for the limiting case of illumination by a purely horizontal radiation field without any azimuthal dependence (case b of Fig. 3), and $W = 1$ for purely vertical illumination (case a of Fig. 3). It is important to point out that the larger the 'anisotropy factor' the larger the fractional atomic polarization that can be induced, and the larger the amplitude of the emergent linear polarization. We choose the positive direction for the Stokes-$Q$ parameter along the X-axis, i.e. along the perpendicular direction to the stellar radius vector through the observed point. The inset shows the wavelength dependence of the anisotropy factor corresponding to the center to limb variation of the observed solar continuum radiation. Note that in this case the maximum anisotropy factor occurs around 2800 Å, i.e., very near the central wavelength of the $k$ line of Mg II, whose polarization may contain valuable information on the magnetic fields of the transition region from the chromosphere to the $10^6$ $K$ solar coronal plasma.

In order to clarify that, depending on the scattering geometry, the Hanle effect can either destroy or create linear polarization in spectral lines, let us consider scattering processes in a $J_l = 0 \rightarrow J_u = 1$ line transition for the following two geometries: 90° scattering and forward scattering.

## 5.1. 90° SCATTERING

Figure 5 illustrates the 90° scattering case, in the absence and in the presence of a magnetic field. For this geometry the largest polarization amplitude occurs for the zero field reference case, with the direction of the linear polarization as indicated in the top panel (i.e, perpendicular to the scattering plane).

    The two lower panels illustrate what happens when the scattering processes take place in the presence of a magnetic field pointing (a) towards the observer (left panel) or (b) away from him/her (right panel). In both situations the polarization amplitude is reduced with respect to the previously discussed unmagnetized case. Moreover, the direction of the linear polarization is rotated with respect to the zero field case. Typically, this rotation is counterclockwise for case (a), but clockwise for case (b)[3]. Therefore, when opposite magnetic polarities coexist within the spatio-temporal resolution element of the observation the direction of the linear polarization is like in the top panel of Fig. 5, simply because the rotation effect cancels out. However, the polarization amplitude is indeed reduced with respect to the zero field reference case, which provides an "observable" that can be used for obtaining empirical information on hidden, mixed polarity fields at subresolution scales in the solar atmosphere (Stenflo, 1982; Trujillo Bueno et al., 2004).
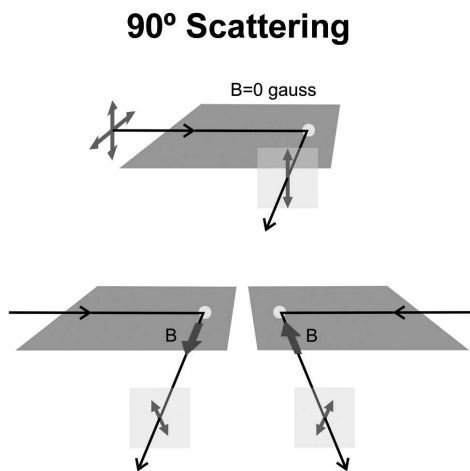
## 90º Scattering



Fig. 5. The 90° scattering case in the absence (top panel) and in the presence (bottom panels) of a deterministic magnetic field.

### 5.2. FORWARD SCATTERING

Figure 6 illustrates the case of forward scattering, in the absence and in the presence of a magnetic field. In this geometry we have *zero* polarization for the unmagnetized reference case, while the largest linear polarization (oriented along the direction of the external magnetic field) is found for "sufficiently strong" fields (i.e., for a magnetic strength such that the ensuing Zeeman splitting is much larger than the level's natural width).

    In other words, in the presence of an *inclined* magnetic field that breaks the symmetry of the scattering polarization problem, forward scattering processes can produce measurable linear polarization signals in spectral lines (Trujillo Bueno, 2001).

---

[3] This occurs when the Landé factor, $g_L$, of the transition's upper level is positive, while the opposite behavior takes place if $g_L < 0$.
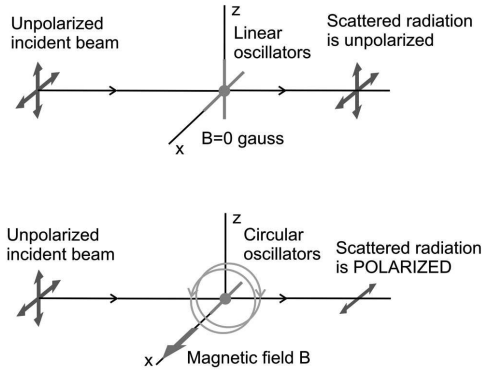
**Forward Scattering**



Fig. 6.   The forward scattering case, in the absence (top panel) and in the presence (bottom panel) of a deterministic magnetic field.

In this case, the linear polarization is created by the Hanle effect, a physical phenomenon that has been clearly demonstrated via spectropolarimetry of solar coronal filaments in the He ɪ 10830 Å multiplet (Trujillo Bueno et al., 2002$a$).

## 6. The Hanle effect: quantum description

As seen in Figs. 5 and 6, the classical description of the Hanle effect is relatively easy to understand (cf., Landi Degl'Innocenti & Landolfi, 2004). In what follows, I provide a very brief explanation within the framework of quantum mechanics, since this is required for a deeper physical understanding of this fascinating effect which has found so many interesting applications in physics (see Moruzzi & Strumia, 1991).

To that end, we need to recall first the concept of quantum coherence ($\rho_J(M, M')$) between different magnetic sublevels $M$ and $M'$ pertaining to each $J$-level. We say that the quantum coherence $\rho_J(M, M')$ is non-zero when the wave function presents a well defined phase relationship between the pure quantum states $|JM\rangle$ and $|JM'\rangle$. It is actually very common to find non-zero coherences while describing the excitation state of an atomic or molecular system under the influence of a pumping radiation field. Let us again consider a two-level atom with $J_l = 0$ and $J_u = 1$ that is being irradiated by an *unpolarized* radiation beam. In the absence of magnetic fields, all coherences of the upper level are zero *if* the quantization axis of total angular momentum is chosen along the symmetry axis of the pumping radiation beam. The same happens if a magnetic field is aligned with the quantization axis and this axis coincides with the symmetry axis of the radiation field that 'illuminates' the atomic system. This is because unpolarized radiation propagating along the quantization axis can only produce *incoherent* excitation of the upper-level sublevels with $M = \pm 1$.[4] If we now rotate the original reference system so that the new quantization

---

[4] Note that an unpolarized radiation beam may be considered as the incoherent superposition of right-handed and left-handed circular polarization.

axis for total angular momentum forms a non-zero angle with the symmetry axis of the radiation field, then non-zero coherences arise in this new reference system, even in the absence of a magnetic field. As shown below in Eq. (6), a magnetic field will relax such quantum coherences.

We thus see that the most general description of the excitation state of a $J$-level requires $(2J + 1)^2$ quantities: the individual populations $(\rho_J(M, M))$ of the $(2J + 1)$ sublevels and the degree of quantum coherence between each pair of them $(\rho_J(M, M'))$. These quantities are nothing but the diagonal and non-diagonal elements of the atomic density matrix associated with the $J$-level, as given by the standard representation. Alternatively, we can use the multipole components $(\rho_Q^K)$ of the atomic density matrix, which are given by linear combinations of $\rho_J(M, M')$. The $\rho_Q^K$ elements with $Q = 0$ are *real* numbers given by linear combinations of the populations of the various Zeeman sublevels corresponding to the level of total angular momentum $J$. The total population of the atomic level $J$ is proportional to $\sqrt{2J + 1}\rho_0^0(J)$, while the population imbalances among the Zeeman sublevels are quantified by $\rho_0^K$ (e.g., $\rho_0^2(J = 1) = (N_1 - 2N_0 + N_{-1})/\sqrt{6}$ and $\rho_0^1(J = 1) = (N_1 - N_{-1})/\sqrt{2}$). However, the $\rho_Q^K$ elements with $Q \neq 0$ are *complex* numbers given by linear combinations of the *coherences* between Zeeman sublevels whose magnetic quantum numbers differ by $Q$ (e.g., $\rho_2^2(J = 1) = \rho(1, -1)$). These multipole components of the atomic density matrix provide the most useful way of quantifying, at the atomic level, the information we need for calculating the *sources* and *sinks* of polarization. Thus, the $\rho_0^0$ elements produce the dominant contribution to the Stokes $I$ parameter, the $\rho_Q^1$ elements (the orientation components) affect the circular polarization, while the $\rho_Q^2$ elements (the alignment components) contribute to the linear polarization signals.

The Hanle effect can be suitably summarized by the following equation, which is valid for the case of a two-level model atom with unpolarized ground level (Landi Degl'Innocenti & Landolfi, 2004):

$$\rho_Q^K(J_u) = \frac{1}{1 + iQ\Gamma_u}[\rho_Q^K(J_u)]_{B=0}, \qquad (6)$$

where $\Gamma_u = 8.79 \times 10^6 \, B \, g_{J_u}/A_{ul}$ and $[\rho_Q^K(J_u)]_{B=0}$ are the $\rho_Q^K$ elements for the non-magnetic case defined in the reference frame in which the quantization axis is aligned with the magnetic field vector. This equation shows clearly that *in the magnetic field reference frame* the population imbalances (i.e., the $\rho_Q^K$ elements with $Q = 0$) are unaffected by the magnetic field, while the $\rho_Q^K$ elements with $Q \neq 0$ are *reduced* and *dephased* with respect to the non-magnetic case. The important point to remember is that the Hanle effect modifies the emergent Stokes profiles because the polarization of the light that is emitted and/or absorbed at each point within the astrophysical plasma under consideration depends sensitively on the local values of the $\rho_Q^K$ elements along the line of sight.

Finally, it is interesting to mention that the Hanle effect (Hanle, 1924) played a fundamental role in the development of quantum mechanics because it led to the introduction and clarification of the concept of *coherent superposition* of pure states. As we have hinted above, the Hanle effect is directly related to the generation of coherent superposition of degenerate Zeeman sublevels of an atom (or molecule) by

a light beam.[5] As the Zeeman sublevels are split by the magnetic field, the degeneracy is lifted and the coherences are modified. This gives rise to a characteristic magnetic-field dependence of the linear polarization of the scattered light that is finding increasing application as a diagnostic tool for magnetic fields in astrophysics (e.g., Asensio Ramos, Landi Degl'Innocenti & Trujillo Bueno, 2005).

## 7. The Paschen-Back effect

As mentioned in Section 2, any atomic level of total angular momentum quantum number $J$ is split by the action of a magnetic field into $(2J + 1)$ equally spaced sublevels, the splitting being proportional to the Landé factor $g_J$ and to the magnetic field strength. This well-known result of first-order perturbation theory is correct only if the splitting produced by the magnetic field on a $J-$level is small compared to the energy separation between the different $J-$levels of the $(L, S)$ term under consideration. In other words, the standard theory of the Zeeman effect is valid only in the limit of "weak" magnetic fields. Here, "weak" means that the coupling of either the spin or the orbital angular momentum to the magnetic field is weaker than the coupling between the spin and the orbital angular momentum (the spin-orbit coupling). This is the so-called Zeeman effect regime.

In the opposite limit, the magnetic field is so "strong" that the spin-orbit interaction can be considered as a perturbation compared to the magnetic interaction. In this case the magnetic field dissolves the fine structure coupling – that is, $\vec{L}$ and $\vec{S}$ are practically decoupled and precess independently around $\vec{B}$. Therefore, the quantum number $J$ loses its meaning. In this so-called complete Paschen-Back effect regime the magnetic Hamiltonian is diagonal on the basis $|LSM_LM_S\rangle$, and the term $(L, S)$ splits into a number of components, each of which corresponds to particular values of $(M_L + 2M_S)$.

Interestingly, since the spin-orbit coupling increases rapidly with increasing nuclear charge, the conditions for a "strong" field are met at a much lower field with light atoms (like helium) than with heavy atoms. For instance, the levels with $J = 2$ and $J = 1$ of the upper term $2^3P$ of the He I 10830 Å multiplet cross for magnetic strengths between 400 G and 1500 G, approximately (e.g., Socas-Navarro, Trujillo Bueno & Landi Degl'Innocenti, 2004). This level-crossing regime corresponds to the incomplete Paschen-Back effect regime, in which the energy eigenvectors are gradually evolving from the form $|LSJM\rangle$ to the form $|LSM_LM_S\rangle$ as the magnetic field increases. This range between the limiting cases of "weak" fields (Zeeman effect regime) and "strong" fields (complete Paschen-Back regime) is more difficult to analyze since it requires a numerical diagonalization of the Hamiltonian.

A particularly interesting phenomenon related to the non-linear effect of the magnetic field on the energy levels in the transition from the Zeeman effect to the complete Paschen-Back effect is the enhancement of the scattering polarization by a vertical magnetic field, which has been investigated by Trujillo Bueno et al. (2002b) for the $D_2$ line of Na I and by Belluzzi, Trujillo Bueno & Landi Degl'Innocenti (2006) for the $D_2$ line of Ba II.

---

[5] A *coherent superposition* of two or more sublevels of a degenerate atomic level is a quantum mechanical state given by a linear combination of pure states of the atomic Hamiltonian.

## 8. Illustrating the effects of the various competing mechanisms on the linear polarization of the He I 10830 Å multiplet

Figure 7 shows theoretical examples of the joint influence of atomic level polarization and the Hanle and Zeeman effects on the emergent Stokes profiles of the He I 10830 Å multiplet, with the wavelength positions and the strengths of the $\pi$ and $\sigma$ transitions calculated within the framework of the incomplete Paschen-Back effect theory. This is shown for a broad range of magnetic field strengths, and for both 90° and forward scattering geometries. We point out that the He I 10830 Å multiplet originates between a lower term ($2^3S_1$) and an upper term ($2^3P_{2,1,0}$). Therefore, it comprises three spectral lines: a 'blue' component at 10829.09 Å (with $J_l = 1$ and $J_u = 0$), and two 'red' components at 10830.25 Å (with $J_u = 1$) and at 10830.34 Å with ($J_u = 2$) which appear blended at solar atmospheric temperatures.

The left panels of Fig. 7 concern the 90° scattering case, which is typical of any off-limb observation. The right panels consider the forward scattering case, which is typical of an on-disk observation at or close to the center of the solar disk. In both cases we have assumed a constant-property slab of optical depth unity at the line center of the red blended component. We have assumed that this slab of helium atoms is located at a height of only 3 arc seconds above the visible solar surface and that it is anisotropically illuminated from below by the photospheric radiation field. The magnetic field is assumed to be horizontal (i.e., parallel to the solar "surface") and oriented in a way such that also for the off-limb case the magnetic field vector is perpendicular to the line of sight. From top to bottom Fig. 7 shows the emergent Stokes $Q$ profile for increasing values of the magnetic strength and for the following three calculations of increasing realism:

(1) The dotted lines indicate the case without atomic level polarization. Here the only mechanism responsible of the emergent linear polarization is the Zeeman splitting of the upper and lower energy levels, which produces wavelength shifts between the $\pi$ and $\sigma$ components, whose positions and strengths have been calculated in the incomplete Paschen-Back effect regime. Therefore, zero polarization is found for $B = 0$ G.

(2) The dashed lines correspond to the case in which we have taken into account the influence of the atomic polarization of the two upper levels of the He I 10830 Å multiplet that can carry atomic level polarization, that is, those with $J = 2$ and $J = 1$. Therefore, in addition to the above-mentioned Zeeman effect contribution, we have here the possibility of a selective emission of polarization components, even for the zero field case. For example, this is the reason why the dashed line of the upper left panel of Fig. 7 shows a non-zero linear polarization signal for the off-limb zero field case.

(3) The solid lines correspond to the most general situation in which the influence of the atomic polarization of the lower level is also taken into consideration, in addition to that of the upper levels and to the Zeeman effect. The consideration of lower-level polarization has two consequences. First, the amount of upper level polarization and the ensuing selective emission of polarization components is modified. Second, we can also have a selective absorption of polarization components. For instance, this is the reason why the blue line of the He I 10830 Å multiplet shows a non-zero linear polarization signal in the $B = 100$ G right panel of Fig. 7.
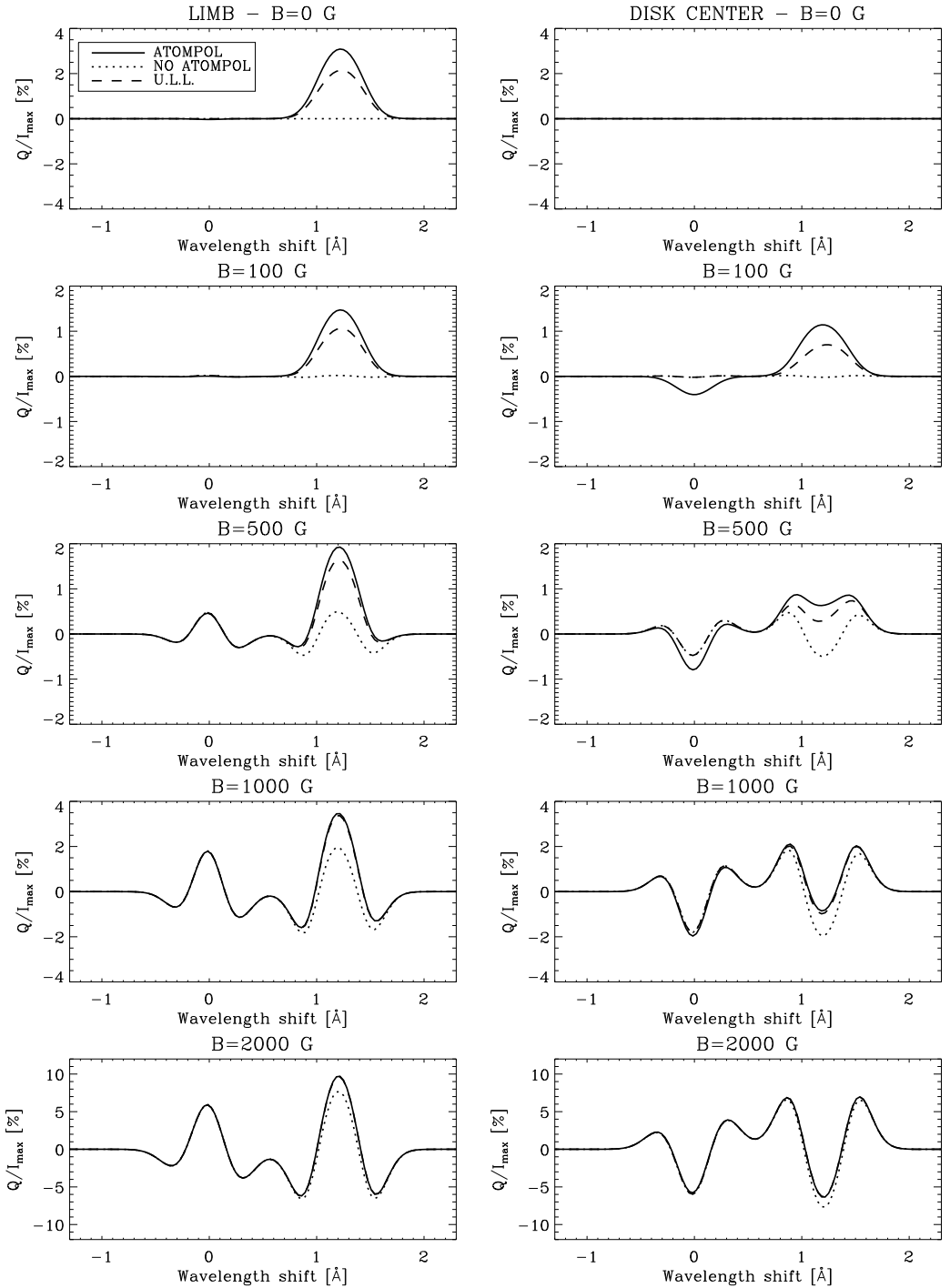
Fig. 7.   Influence of atomic level polarization on the emergent linear polarization of the He I 10830 Å multiplet. See the text for details. The positive reference direction for Stokes $Q$ is along the direction of the horizontal magnetic field. From Trujillo Bueno & Asensio Ramos (2007).

As shown in Fig. 7, for weak magnetic fields (e.g., $B \leq 100$ G) the emergent linear polarization is fully dominated by the *selective emission* and *selective absorption* of polarization components that result from the atomic level polarization induced by the anisotropic illumination of the slab's helium atoms (Trujillo Bueno et al., 2002*a*). For stronger magnetic fields, the contribution of the transverse Zeeman effect cannot be neglected. However, the emergent linear polarization may still show an important contribution caused by the presence of atomic level polarization, even for magnetic strengths as large as 1000 G. Interestingly, the observational signature of this atomic level polarization is clearly seen in many of the Stokes $Q$ and $U$ profiles that some observers have measured in emerging magnetic flux regions, even at points of the observed field of view for which magnetic strengths as large as 1000 G are inferred (see details in Trujillo Bueno & Asensio Ramos, 2007). Therefore, the modeling of the Stokes $Q$ and $U$ profiles of the spectral lines of the He I 10830 Å multiplet should *not* be done by taking only into account the contribution of the transverse Zeeman effect, unless the magnetic field intensity of the observed plasma structure is sensibly larger than 1000 G.

## 9. Summarizing: Zeeman vs. Hanle

The good news about the Zeeman effect is that the mere detection of polarization implies the presence of a magnetic field. The bad news are the following:

— It is of limited practical interest for the determination of magnetic fields in hot coronal plasmas because the Zeeman polarization scales with the ratio between the Zeeman splitting and the Doppler-broadened line width.

— The Zeeman effect is "blind" to magnetic fields that are tangled on scales too small to be resolved.

Concerning the Hanle effect, these are the good news:

— It is sensitive to magnetic fields for which the Zeeman splitting in frequency units is comparable to the inverse lifetime of the upper (or lower) level of the spectral line used, regardless of how large the line width due to Doppler broadening is. It is therefore sensitive to weaker magnetic fields than the Zeeman effect: from at least milligauss to hundreds of gauss.

— It is sensitive to the presence of hidden, mixed-polarity fields at sub-resolution scales.

— Contrary to a widespread belief, the diagnostic use of the Hanle effect is *not* limited to a narrow solar limb zone. In particular, in forward scattering at disk center, the Hanle effect can create linear polarization, when in the presence of inclined magnetic fields.

The downside of the Hanle effect is that it is properly a quantum effect, and the quantum theory of polarization is a complicated subject. However, it has been recently described in great detail in a rigorous monograph (see Landi Degl'Innocenti & Landolfi, 2004). And we know how to solve the relevant equations accurately and efficiently in order to model polarization phenomena in (magnetized) astrophysical plasmas (Trujillo Bueno, 2003*b*; see also the multilevel radiative transfer code of Manso Sainz & Trujillo Bueno, 2003*b*).

## 10. Concluding remarks

Polarized light provides the most reliable source of information at our disposal for the remote sensing of astrophysical magnetic fields, including those on the Sun. However, in order to open a true empirical window on solar and stellar magnetism, we need to develop and apply suitable diagnostic tools that take proper account of the various physical mechanisms that produce polarization in spectral lines. Hopefully, the brief introduction provided here will motivate the reader to go deeper into the subject.

## References

Asensio Ramos, A., Landi Degl'Innocenti, E., Trujillo Bueno, J. 2005, ApJ, **625**, 985

Belluzzi, L., Trujillo Bueno, J., Landi Degl'Innocenti E, 2006, in Solar Polarization 4, eds. R. Casini & B. Lites, ASP Conf. Series, in press

Born, M., & Wolf, E. 1994, *Principles of Optics*, Pergamon Press, Oxford

Condon, E.U., & Shortley, G.H. 1935, *The Theory of Atomic Spectra*, Cambridge University Press, Cambridge

Gandorfer, A. 2000, *The Second Solar Spectrum*, Vol. 1: 4625 Å to 6995 Å ISBN 3 7281 2764 7 (Zürich: vdf)

Gandorfer, A. 2002, *The Second Solar Spectrum*, Vol. 2: 3910 Å to 4630 Å ISBN 3 7281 2855 4 (Zürich: vdf)

Hanle, W. 1924, Z. Phys., **30**, 93

Happer, W. 1972, Rev. Mod. Phys., **44**, 169

Kastler, A. 1950, J. de Physique, **11**, 255

Landi Degl'Innocenti, E., Landolfi, M. 2004, *Polarization in Spectral Lines*, Kluwer Academic Publishers

Manso Sainz, R., Trujillo Bueno, J. 2003*a*, Phys. Rev. Letters, **91**, 111102-1

Manso Sainz, R., Trujillo Bueno, J. 2003*b*, in Solar Polarization 3, eds. J. Trujillo Bueno & J. Sánchez Almeida, ASP Conf. Series **307**, 251

Moruzzi, G., Strumia, F. (eds.) 1991, *The Hanle Effect and Level-Crossing Spectroscopy*, New York: Plenum

Socas-Navarro, H., Trujillo Bueno, J., & Landi Degl'Innocenti, E. 2004, ApJ, **612**, 1175

Stenflo, J.O. 1982, Solar Phys., **80**, 209

Stenflo, J.O. 2002, in *Astrophysical Spectropolarimetry*, J. Trujillo Bueno, F. Moreno-Insertis & F. Sánchez (eds.), Cambridge University Press, 55

Stenflo, J.O., & Keller, C. 1997, A&A, **321**, 927

Stenflo, J.O., Keller, C., & Gandorfer, A. 2000, A&A, **355**, 789

Trujillo Bueno, J. 1999, in Solar Polarization, eds. K. N. Nagendra and J. O. Stenflo, Kluwer Academic Publishers, 73

Trujillo Bueno, J. 2001, in Advanced Solar Polarimetry: Theory, Observation and Instrumentation, ed. M. Sigwarth, ASP Conf. Series **236**, 161

Trujillo Bueno, J. 2003*a*, in Solar Polarization 3, eds. J. Trujillo Bueno & J. Sánchez Almeida, ASP Conf. Series **307**, 407

Trujillo Bueno, J. 2003*b*, in Stellar Atmosphere Modeling, eds. I. Hubeny, D. Mihalas and K. Werner, ASP Conf. Series **288**, 551

Trujillo Bueno, J., Landi Degl'Innocenti, E. 1997, ApJ Letters, **482**, L183

Trujillo Bueno, J., Asensio Ramos, A. 2007, ApJ, **655**, 642

Trujillo Bueno, J., Landi Degl'Innocenti, E., Collados, M., Merenda, L. & Manso Sainz, R. 2002*a*, Nature, **415**, 403

Trujillo Bueno, J., Casini, R., Landolfi, M., Landi Degl'Innocenti, E. 2002*b*, ApJ Letters, **566**, L53

Trujillo Bueno, J., Shchukina, N., Asensio Ramos, A. 2004, Nature, **430**, 326